

Advancing the High Throughput Identification of Liver Fibrosis Protein Signatures Using Multiplexed Ion Mobility Spectrometry*[§]

Erin Shammel Baker‡|||, Kristin E. Burnum-Johnson‡|||, Jon M. Jacobs‡|||, Deborah L. Diamond§, Roslyn N. Brown‡, Yehia M. Ibrahim‡, Daniel J. Orton‡, Paul D. Piehowski‡, David E. Purdy¶, Ronald J. Moore‡, William F. Danielson, III‡, Matthew E. Monroe‡, Kevin L. Crowell‡, Gordon W. Slys‡, Marina A. Gritsenko‡, John D. Sandoval‡, Brian L. LaMarche‡, Melissa M. Matzke‡, Bobbie-Jo M. Webb-Robertson‡, Brenna C. Simons§§, Brian J. McMahon§§, Renuka Bhattacharya||, James D. Perkins**, Robert L. Carithers, Jr.¶, Susan Strom||, Steven G. Self‡‡, Michael G. Katze¶, Gordon A. Anderson‡, and Richard D. Smith‡¶¶

Rapid diagnosis of disease states using less invasive, safer, and more clinically acceptable approaches than presently employed is a crucial direction for the field of medicine. While MS-based proteomics approaches have attempted to meet these objectives, challenges such as the enormous dynamic range of protein concentrations in clinically relevant biofluid samples coupled with the need to address human biodiversity have slowed their employment. Herein, we report on the use of a new instrumental platform that addresses these challenges by coupling technical advances in rapid gas phase multiplexed ion mobility spectrometry separations with liquid chromatography and MS to dramatically increase measurement sensitivity and throughput, further enabling future high throughput

MS-based clinical applications. An initial application of the liquid chromatography - ion mobility spectrometry-MS platform analyzing blood serum samples from 60 postliver transplant patients with recurrent fibrosis progression and 60 nontransplant patients illustrates its potential utility for disease characterization. *Molecular & Cellular Proteomics* 13: 10.1074/mcp.M113.034595, 1119–1127, 2014.

To date pre-clinical and clinical applications of MS-based proteomic techniques analyzing complex biofluids have fallen short of expectations, largely due to deficiencies in both analytical sensitivity and throughput. These deficiencies result in measurements typically failing to confidently detect and quantify proteins at moderate to low concentrations, or not providing sufficient sample analysis throughput for statistical relevance. Targeted MS analyses with higher sensitivity are currently utilized to address these shortcomings (1, 2); however, these studies often only analyze a small list of proteins identified as biologically significant. While targeted MS measurements are increasingly common in clinical applications (3, 4), the limited number of proteins they examine does not necessarily reflect the biodiversity across a population, making broad untargeted measurements essential in developing individual disease metrics for diagnosis (5). As the future of medicine proceeds toward a personal profiling approach (6, 7), the potential for robust high throughput clinical measurements based upon MS is highly attractive, though only if its deficiencies can be addressed.

An initial step in attaining broad untargeted measurements that increasingly retain the benefits of targeted analyses exploits technological advances such as faster separations, more effective ion sources, detectors with greater dynamic range, and MS measurements with both higher resolution and accuracy. Advanced liquid-phase separations have already

From the ‡Biological Sciences Division and Environmental Molecular Sciences Laboratory, Pacific Northwest National Laboratory, Richland, Washington; §Department of Pharmaceutics, University of Washington, Seattle, Washington; ¶Department of Microbiology, School of Medicine, University of Washington, Seattle, Washington; ||Division of Gastroenterology, Department of Medicine, University of Washington, Seattle, Washington; **Division of Transplantation, Department of Surgery, University of Washington, Seattle, Washington; ‡‡Vaccine and Infectious Disease Division, Fred Hutchinson Cancer Research Center, Seattle, Washington; §§Alaska Native Tribal Health Consortium, Liver Disease and Hepatitis Program, Anchorage, Alaska

Received September 23, 2013, and in revised form, January 7, 2014

Published, MCP Papers in Press, January 8, 2014, DOI 10.1074/mcp.M113.034595

Author contributions: E.S.B., K.E.B., J.M.J., R.B., J.D.P., R.L.C., S.S., and S.G.S. designed research; E.S.B., R.N.B., P.D.P., D.E.P., M.A.G., B.C.S., and B.J.M. performed research; E.S.B., Y.M.I., D.J.O., R.J.M., W.F.D., B.L.L., and R.D.S. contributed new reagents or analytic tools; E.S.B., K.E.B., J.M.J., D.L.D., M.E.M., K.L.C., G.W.S., J.D.S., M.M.M., and B.M.W. analyzed data; E.S.B., K.E.B., and J.M.J. wrote the paper; B.J.M., G.A.A., and R.D.S. managed parts of project; M.G.K. managed parts of research.

been employed to provide a significant sensitivity increase as illustrated by the higher number of proteins detected in liquid chromatography (LC)¹-MS-based studies (8), however, the long LC separations most compatible with blood samples are extremely time-consuming. Fast gas-phase ion mobility spectrometry (IMS) separations that take place on the time scale of tens of milliseconds offer an additional separation stage and a way of reducing the need for extended LC separation times. In an IMS separation, ions subjected to an electric field while traveling through a buffer gas separate quickly based on ion shape, for example, compact species drift faster than those with extended structures (9, 10). IMS can be coupled between LC and orthogonal acceleration time-of-flight (TOF) MS stages. By combining these three orthogonal separations into a single LC-IMS-MS instrumentation platform, multidimensional high-resolution nested spectra are produced containing elution times, mass-to-charge ratios (m/z) and IMS drift times for all detectable ions in a sample (11, 12). The objective of this manuscript is to evaluate an LC-IMS-MS platform performance against an LC-MS only platform and determine how well it performs with clinical samples.

EXPERIMENTAL PROCEDURES

LC-IMS-MS and LC-MS—Analysis of the 120 human serum samples was performed on an in-house built instrument that couples a 1-m ion mobility separation with an Agilent 6224 TOF MS upgraded to a 1.5 meter flight tube providing resolution of ~25,000 in enhanced dynamic range mode (12). The analysis of the spiked peptide samples and a small subset of the human serum samples was performed on both a Thermo Fisher Scientific LTQ Orbitrap Velos MS (Velos) (San Jose, CA, USA) operated in tandem MS (MS/MS) mode and the in-house built IMS-MS instrument. A fully automated in-house built 4-column HPLC system equipped with in-house packed capillary columns was used for both instruments with mobile phase A consisting of 0.1% formic acid in water and phase B comprised of 0.1% formic acid in acetonitrile (13). A 100-min LC gradient was performed on the LTQ Orbitrap Velos MS (using 60 cm long columns with an o.d. of 360 μm , i.d. of 75 μm , and 3- μm C₁₈ packing material), whereas only a 60-min gradient with shorter columns (30 cm long with same dimensions and packing) was used with the IMS-MS. Both gradients increased mobile phase B from 0 to 60% until the final 2-min of the run when B was purged at 95%. 5 μl of each sample was injected for both analyses and the HPLC was operated under a constant flow rate of 0.4 $\mu\text{l}/\text{min}$ for the 100-min gradient and 1 $\mu\text{l}/\text{min}$ for the 60-min

gradient. The Velos MS data were collected from 400–2000 m/z at a resolution of 60,000 (automatic gain control (AGC) target: 1×10^6). IMS-MS data were collected from 100–3200 m/z .

Additional Methods—Detailed descriptions of the sample preparation, nanoHPLC, mass spectrometry, informatics approach and statistical analysis are available in Supplemental Methods.

RESULTS

IMS-MS Developments and Improvements to Increase Sensitivity and Duty Cycle—Practical use of IMS-MS was initially impeded by its low sensitivity due to significant ion losses at the IMS drift cell termini. This problem was solved with ion funnels by re-focusing both the ions exiting the source and those leaving the drift cell (Fig. 1A), making the addition of the IMS stage essentially lossless (14). However, the use of both efficient ion sources and interfaces with efficient ion accumulation between injections is problematic due to space charge constraints. Another limitation that has hindered widespread use of IMS-MS is its inherent low duty cycle. During traditional IMS experiments, ions are only pulsed into the drift cell after all ions from the previous packet exit, resulting in utilization of only a small percentage of the ions created in the source. To address this constraint, a multiplexing approach based on the Hadamard transform was developed so that discreet packets of ions could co-exist in the drift cell as long as they did not overlap due to diffusional broadening (Fig. 1B and 1C) (15). This approach substantially circumvents space charge limitations, allows much higher IMS duty cycle, significantly increases measurement sensitivity, and deconvolution of its pseudorandom sequence has been shown to greatly reduce the noise in the spectra allowing a much higher signal to noise ratio for the resulting ions (16). These improvements in addition to the reduced spectral congestion from the IMS separation have enabled faster LC gradient times, thereby increasing analyses throughput (12). To take advantage of the faster sample analyses and higher sensitivity measurements, we developed a LC-IMS-MS analytical platform with the above sensitivity improvements for application to clinically focused large-scale proteomic measurements.

LC-IMS-MS Platform Evaluation and Validation—In an initial evaluation of the new LC-IMS-MS platform, its performance was compared with an LC-MS platform (comprised of a commercially available LTQ Orbitrap Velos). Nine blood serum samples were analyzed on each platform, and a 100-min LC gradient was used for LC-MS, whereas a 60-min LC gradient was used for LC-IMS-MS. Even with the shorter analysis time, >20% more deisotoped spectral features (putative peptides) were detected with the LC-IMS-MS platform compared with the LC-MS platform (Fig. 1D), an observation attributed to the reduced spectral congestion from the additional IMS separation and the higher signal to noise ratios from multiplexing. These attributes allow detection of additional proteins not seen in the LC-MS experiments and additional coverage and confidence for peptides observed with significant differential abundance in the LC-IMS-MS analyses. To further under-

¹ The abbreviations used are: MS, mass spectrometry; IMS, ion mobility spectrometry; LC, liquid chromatography; TOF, time-of-flight; m/z , mass-to-charge ratios; HCV, Hepatitis C Virus; NP, non-progressors; SP, slow progressors; FP, fast progressors; C4A, complement component 4A; ECM1, extracellular matrix proteins; LGALS3BP, galectin-3-binding protein; ACTB, cytoskeletal β -actin; TGFBI, transforming growth factor- β -induced protein ig-h3; F12, coagulation factor XII; TGF- β 1, transforming growth factor β ; VTN, vitronectin; LUM, lumican; F10, coagulation factor X; C5, complement factor 5; A1BG, alpha-1B-glycoprotein; CFH, complement factor H; IGFALS, insulin-like growth factor-binding protein complex acid labile subunit; PROC, vitamin K-dependent protein C; RBP4, retinol-binding protein 4; HPX, hemopexin; A2M, alpha-2-macroglobulin; F2, Prothrombin; QSOX1, sulfhydryl oxidase 1.

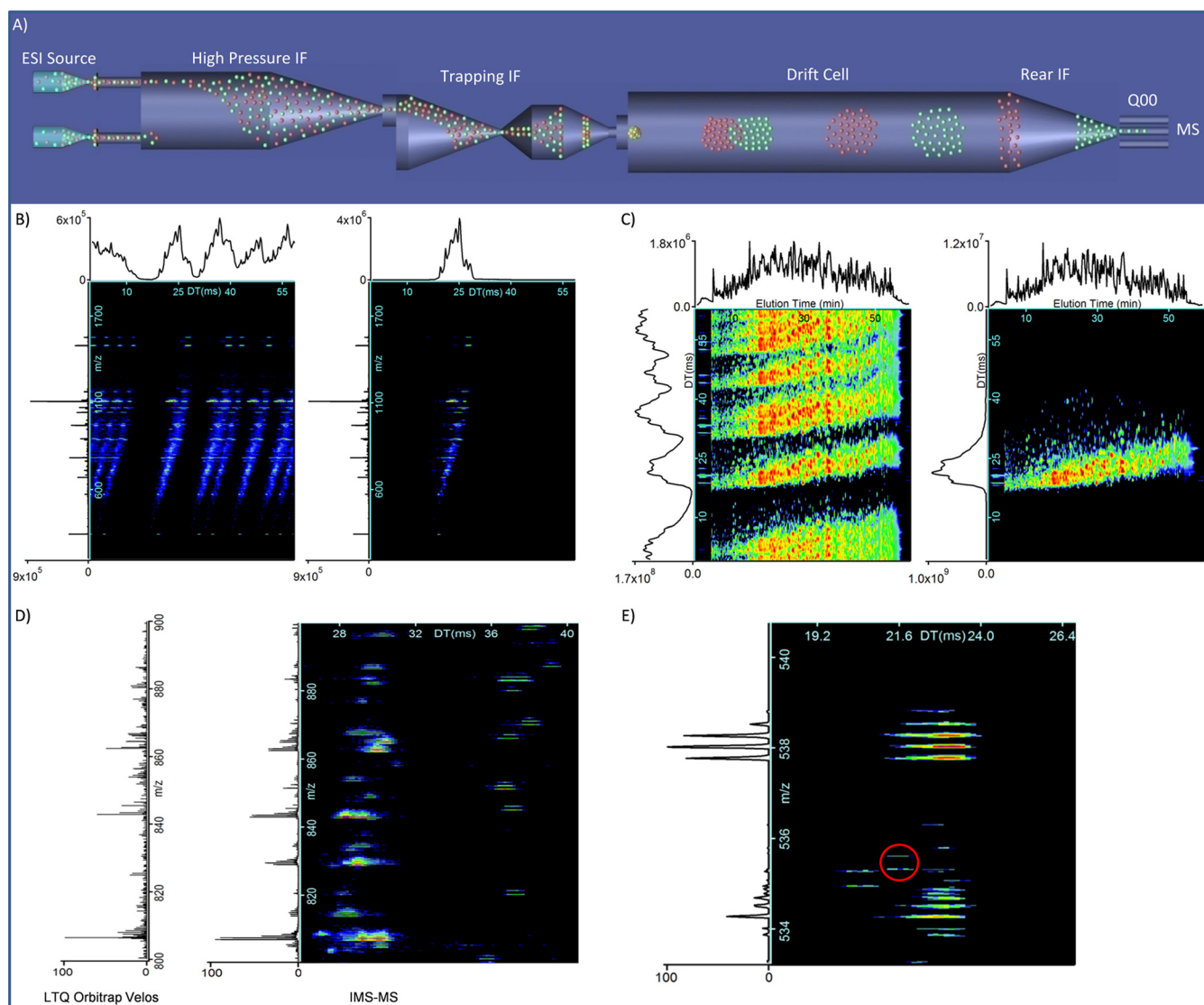


FIG. 1. **A**, A schematic representation of the ESI-IMS-MS platform with the smaller (green) and larger (red) conformational ions illustrating size separation in the IMS drift cell. **B**, Multiplexed (left) and de-multiplexed (right) nested IMS spectra show both IMS drift time (x axis) and m/z (y axis) for a 9 peptide mixture where 8 ion packets were released into the drift cell simultaneously. **C**, Since LC adds a third dimension to LC-IMS-MS analyses, additional plots are necessary to illustrate the LC total ion chromatogram (x axis) and IMS drift time (y axis) for a human serum dataset before (left) and after (right) de-multiplexing. **D**, MS spectra for the LTQ Orbitrap Velos (left) and IMS-MS (right) illustrate noise reduction in the IMS-MS spectrum and how additional drift time information greatly simplifies peak detection ultimately leading to more identifications. **E**, (Dynorphin A porcine)³⁺ spiked at 100 pg/ml into human serum is circled in the LC-IMS-MS spectrum. Intensity in the spectra for **B**, **C**, **D**, and **E** is represented by color (red being the most intense and blue the least on a logarithmic scale).

stand why more features were observed in the LC-IMS-MS platform even with a reduced LC gradient, a follow-up limit of detection study was performed and involved both platforms analyzing three technical replicates of a normal human serum sample spiked with eight nonhuman peptides ranging in concentrations from 100 pg/ml to 100 ng/ml. Overall, the LC-IMS-MS platform detected peptides at concentrations $\sim 100\times$ lower than the LC-MS platform with a linear correlation to concentrations, lower coefficient of variation (CV) values and modestly higher throughput (60-min *versus* 100-min) as shown by Table I and Fig. 1E. These advantages

illustrate the potential gains in enhanced dynamic range, proteome coverage, and increased speed for the LC-IMS-MS platform. To allow direct comparison of the TOF MS (60-min LC separation) and LTQ Orbitrap Velos (100-min separation), the IMS drift cell was removed. Both instruments illustrated similar limits of detection (Table I) illustrating that the increased measurement sensitivity observed with the LC-IMS-MS platform can be attributed specifically to the IMS separation.

To more fully evaluate the applicability of the LC-IMS-MS platform, we utilized it in a study involving patients affected

TABLE I

Scaled abundance and coefficient of variation (CV) values for eight nonhuman peptides spiked into human serum for 60-min LC-IMS-TOF MS, 60-min LC-TOF MS, and 100-min LC-LTQ Orbitrap Velos analyses

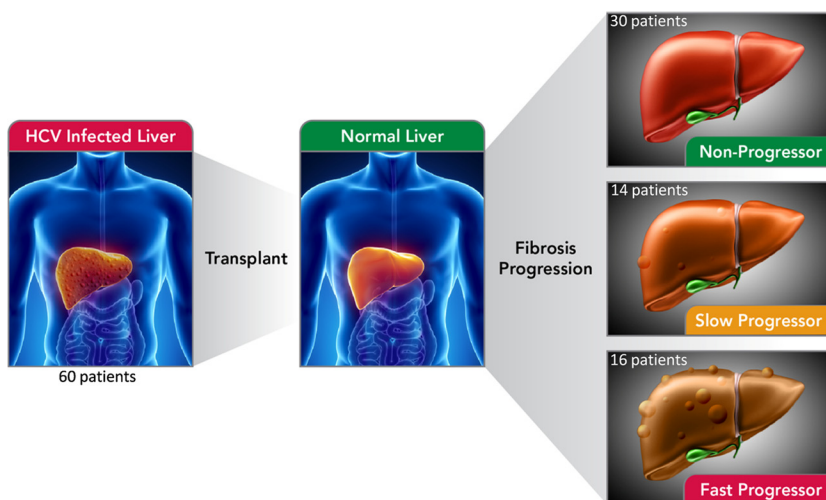
Spiking Level	Peptide	Neutral Mass	Most Abundant Charge State(s)	Peptide Scaled Abundance ^a and CV Values ^{b,c}		
				60-min LC-IMS-TOF MS	60-min LC-TOF MS	100-min LC-LTQ Orbitrap Velos
100 pg/ml	Melittin	2844.75	4, 5	ND	ND	ND
100 pg/ml	Dynorphin A Porcine (Frag 1–13)	1602.98	3	1.7 (18)	ND	ND
1 ng/ml	Des Pro Ala Bradykinin	920.50	2	21 (12)	ND	ND
1 ng/ml	Leucine Enkephalin	555.27	1	23 (10)	ND	ND
10 ng/ml	3X FLAG Peptide	2860.14	5	115 (8)	125 (20)	ND
10 ng/ml	Substance P	1346.73	2	126 (7)	138 (18)	112 (19)
100 ng/ml	[Ala92]-Peptide 6	2122.18	4	868 (4)	848 (11)	841 (12)
100 ng/ml	Methionine Enkephalin	573.23	1	1000 (3)	1000 (9)	1000 (10)

^a Peptide abundance values from 3 datasets were averaged and re-scaled to a range of 0 to 1000 for direct instrument comparison (by dividing the most abundant peptide value in each instrument and multiplying by 1000).

^b CV values are in parenthesis.

^c ND = not detected.

FIG. 2. Blood samples from 60 HCV patients following liver transplant were utilized in this study. Based on the amount of fibrosis occurring in their liver several months to a few years following the procedure, the patients were categorized into non-, slow or fast fibrosis progressor groups. A biostatistician selected patients for the study so that a nonprogressor patient could be matched to either a slow or fast progressor, resulting in 30 well-annotated patient pairs.



with chronic hepatitis C virus (HCV). HCV represents a worldwide public health concern affecting an estimated 130–170 million people (17) and is the leading cause of liver transplants in the United States and Europe causing a major burden on healthcare services (18, 19). In this disease, the liver elicits a persistent inflammatory and repair response known as fibrosis, which is characterized by the formation of fibrous tissue and scarring on the liver. Because the prognosis of HCV patients is related to the development of fibrosis and the risk of cirrhosis and hepatocellular carcinoma, an accurate evaluation of fibrogenic progression is important for patient care. Currently, liver biopsies represent the primary technique for generating accurate information on the degree of fibrosis; however, they have multiple disadvantages, including risk of complications (*i.e.* major bleeding or inadvertent puncture of the lung, kidney, or colon), cost and occasionally inaccurate findings due to small specimen size and variability in the histology evaluation. These disadvantages have spurred the development of noninvasive methods that can reliably predict, diagnose and assess the degree of fibrosis (20, 21).

In this study, blood serum samples chosen from 60 HCV patients following liver transplantation at the University of Washington Medical Center were initially utilized to evaluate the LC-IMS-MS platform for clinical use (Fig. 2). These 60 samples represented 30 patients termed nonprogressors (NP) who showed no or mild return of fibrosis over a range of times postliver transplant (2 to 4 years), compared with 30 patients who developed “stage 3 to 4” fibrosis over a similar period of time and were stratified into either slow progressors (SP; stage 3–4 fibrosis at 3–4 years posttransplant) or fast progressors (FP; stage 3–4 fibrosis within 2 years posttransplant). The degree of fibrosis in these transplant patients was scored from 0 to 4 utilizing the Batts-Ludwig scoring system, and the serum samples were collected at a specific time point posttransplant (See supplemental Table S1 and Supplemental transplant sample data). Using a multivariate approach, patients were matched for donor age, cold ischemia time of the transplanted organ and time to biopsy, which are the most important clinical variables known to influence the risk of fibrosis progression associated with recurrent hepatitis C after liver transplantation. Final matching resulted in 30

patient pairs (progressor *versus* nonprogressor) and all samples were analyzed as technical replicates utilizing the LC-IMS-MS platform for global proteome evaluation of each patient sample.

Statistical Trends for Proteins with Significant Differential Abundance Discriminating between Fibrosis Conditions—Following data acquisition of the 60 HCV liver transplant serum samples with LC-IMS-MS, overall statistical significance was assessed. Initially, peptides distinguishing NP, SP, and FP conditions with significant differential abundance were analyzed and then protein significance was evaluated by merging these peptides. To determine the significance of the peptides, PNNL's DANTE software was utilized to convert the peak intensity values to a log₂ scale and statistically compare them utilizing ANOVA for generation of p- and q-values (22). Our analysis only focused on significantly changing peptides with q-values <0.05 to reduce false positives, and these were rolled into proteins using DANTE's Rollup parameters (reference peptide based scaling). Statistical comparisons were also done at the protein level and a protein was only considered significant if it had at least two peptide identifications. In the LC-IMS-MS data, statistical analysis revealed 136 proteins with significant differential abundances in the serum of transplant patients. Of these, 112 proteins were observed to discriminate between the NP and FP patient groups and 101 between NP and SP patient groups, with 77 overlapping as illustrated in Fig. 3a (see [supplemental Tables S1–S5](#) for detailed protein and peptide tables).

Functional Classification and Comparison with Previous Finding—Serum results were functionally classified, focusing on mechanisms most relevant for comparisons within liver function: liver metabolism, immune response (innate and adaptive), oxidative stress, liver fibrosis, and secreted effectors ([supplemental Table S5](#), Fig. 3B). General trends revealed that patients with fibrosis had a decrease in liver metabolism serum level markers and an increase in oxidative stress markers (as seen previously in (23)). Mechanistically, this reflects a reduction in gross metabolism, in line with attenuation of liver function, but appears to do so under significant oxidative stress resulting in the production of stress response proteins. As with any comprehensive serum/plasma protein study, multiple signature immune proteins were also captured, including alterations in adaptive immunoglobulin responses, acute phase and inflammatory markers, and the complement pathway. Though likely not specific as markers of fibrosis progression, these signatures still reflect the gross alterations visible in this biofluid as a direct result of liver injury. Of specific relevance to HCV infection, however, is complement component 4A (C4A) which exhibited lower abundance in the SP and FP patient groups, consistent with recent papers that have shown it has significantly lower activity in HCV infected patients due to transcriptional repression by HCV proteins (24, 25).

Interesting trends were observed in the panel of liver fibrosis proteins allowing for differentiation of the NP, SP, and FP patient groups. Extracellular matrix proteins such as ECM1 and galectin-3-binding protein (LGALS3BP), which contribute to the collagenous matrix of the fibrotic tissue in chronic hepatic fibrosis, both increased in SP and FP patient groups, as well as cytoskeletal β -actin (ACTB) which has been shown to increase in a radiation induced skin and muscular fibrosis study (26). A significant increase was observed in FP patients for transforming growth factor- β -induced protein ig-h3 (TGFB1) and coagulation factor XII (F12). Because TGFB1 is associated with transforming growth factor β (TGF- β 1), a multifunctional cytokine linked to several pathological processes including tissue fibrosis, and studies have shown that F12 expression is induced by TGF- β 1 in human lung fibroblasts (27), their direct upward correlation in FP patients makes sense. Finally, differential responses were observed in some protein markers such as vitronectin (VTN), lumican (LUM), coagulation factor X (F10) and complement factor 5 (C5), which decrease in SP, but increase in FP. F10 and C5 have been shown to drive the fibrotic response in human lung and liver fibrogenesis (28, 29) and because both proteins are elevated in FP serum and have documented causal roles in fibrogenesis, they may now be viewed as key potential indicators of the rapid pathological decline seen in transplanted livers of FP patients.

The current LC-IMS-MS platform serum findings also overlapped exceptionally well with previously reported and validated promising biomarkers for HCV progression from other serum studies. Five proteins (A1BG, CFH, IGFALS, PROC, and RBP4) were identified and verified with selected reaction monitoring as potential serum biomarkers that separate HCV-infected patients from healthy individuals or distinguish HCV patients at different stages of fibrosis (30). All five proteins were detected with significant differential abundance in our analysis, and observed with the same expression trends. Additionally, markers such as C4A (24, 25), LGALS3BP (31), HPX (32), A2M (32) have also been reported previously, and overlap with the current findings, as well as a vast majority of the serum proteins observed with significant differential abundance in a nonalcoholic fatty liver disease study (33). Due to the high sensitivity of the LC-IMS-MS measurements, we were able to detect significance of many proteins simultaneously that have only been observed as subsets in prior manuscripts.

Nontransplant Patient Serum Verification Analysis and Comparison—Investigations utilizing a liver transplant patient population confer multiple advantages in studies involving fibrosis progression. However, it is recognized that such studies also introduce clinical confounders and variables not mechanistically linked to progression of liver fibrosis but directly related to the transplantation itself and immunosuppressive environments. To provide clarity toward significant findings from our transplant model and at the same time verify

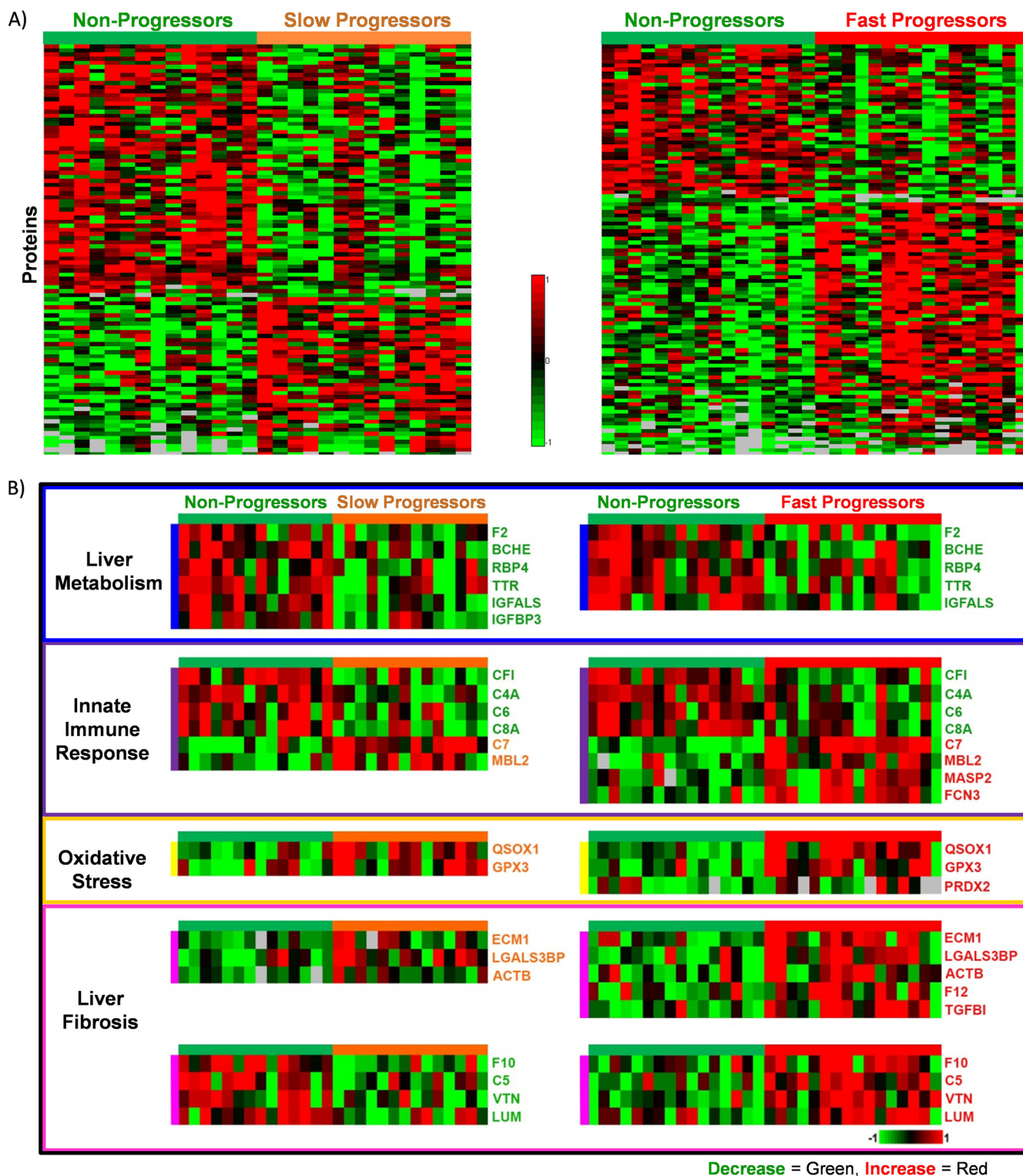
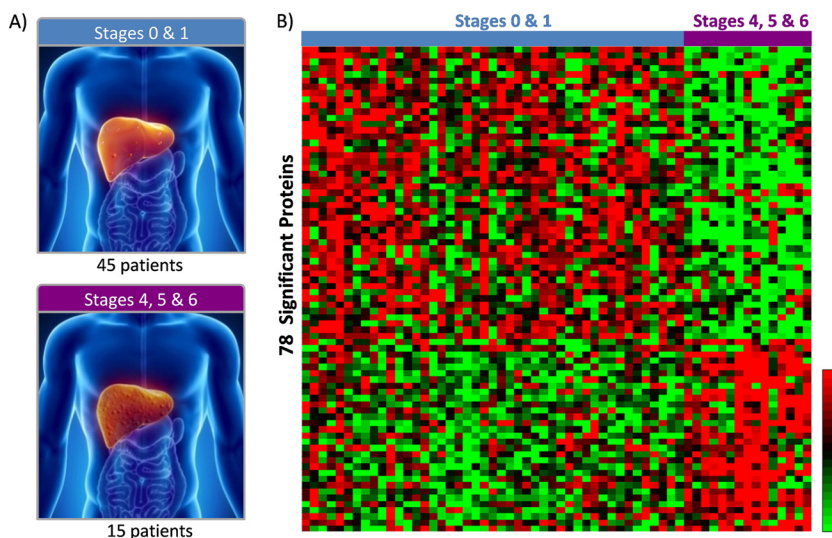


FIG. 3. **A**, Heat maps representing the relative \log_2 intensity change for proteins with significant differential abundance when nonprogressors are compared with either slow (left) or fast progressors (right). Each column represents one of the 60 patients and each row one of the significant proteins. Trends between the patient groups are clearly observed, but biodiversity in the human population is also discerned. **B**, The proteins with significant differential abundance were further characterized into four groups: liver metabolism, innate immune response, oxidative stress or liver fibrosis. Twenty-six selected proteins are shown to illustrate the trend of each category where the gene names given in UniProtKB are used as abbreviated protein names. Decrease in relative abundance is shown by green and increase by red (missing values are shown as gray).

FIG. 4. **A**, Blood samples from 60 HCV infected nontransplant patients were utilized for comparison and validation of the transplant patient results. Patients were categorized into two categories, low fibrosis stages 0 and 1 and high fibrosis stages 4, 5, and 6. **B**, Heat maps illustrating the relative log₂ intensity change for differential proteins from the nontransplant patient groups. Each column represents one of the 60 patient and each row one of the 78 significant proteins. Decrease in relative abundance is shown by green and increase by red.



the subset of detected serum proteins which are directly related to fibrosis progression, we utilized the same LC-IMS-MS platform to survey a completely independent HCV-infected but nontransplant patient group available through the Alaska Hepatitis C Cohort. A total of 60 patient serum samples were identified and analyzed based upon fibrosis stratification of Ishak score 0–1 *versus* 4–6, with a timeframe of sampling within 6 months of a diagnostic biopsy as shown in Fig. 4A (see supplemental Table S6 and Supplemental non-transplant sample data for details). Statistical analysis of the subsequent peptide and protein results was performed using an independent analysis pipeline (See supplemental Tables S6–S9 and supplemental Methods for details) which resulted in the orthogonal identification of 78 proteins which differentiate between the fibrosis classes (Fig. 4B). Notably, 63 of these proteins (81%) overlap with those that significantly differentiate fibrosis progression in the initial transplant patient results. After excluding the 4 transplant proteins which decrease in SP, but increase in FP, >91% are observed with common abundance directionality, providing a strong orthogonal validation of core proteins based upon both transplant and nontransplant studies. Furthermore, of the 15 proteins uniquely significant in the nontransplant data, half have supporting significant peptides in the transplant data, but were excluded due to lack of multiple peptides per protein. (See supplemental Table S9C for protein overlap information).

To provide further validation of the results from the LC-IMS-MS platform, a subset of Western blot immunoassays were performed on five proteins with significant differential abundance in both the transplant and nontransplant patients groups (F2, C4A, QSOX1, ECM1, and LGALS3BP). Within the LC-IMS-MS studies, F2 and C4A both decrease in patients with fibrosis while QSOX1, ECM1, and LGALS3BP increase. These results were essentially mirrored in the immunoassay blot results where two transplant NP-FP patient pair serum samples were blotted for each protein as shown in Fig. 5.

Corresponding bar graphs representing the LC-IMS-MS measured protein values are also shown in Fig. 5. The Western blots provided orthogonal validation of the LC-IMS-MS platform with both techniques showing good agreement for all five proteins.

DISCUSSION

Overall, the experiments performed in this manuscript illustrate that the multidimensional LC-IMS-MS platform greatly improves upon existing MS technologies in analytical sensitivity and specificity, enhances dynamic range of measurements, and provides reliable identification and quantitation of low abundance analyte species in highly complex biological matrices. Additionally the enhanced throughput of the new platform highlights the ability of this technology for pursuing large clinical-based global studies. Though we fully expect continued sensitivity and throughput advancements, the development and demonstration of the current platform sets a key foundational benchmark for further efforts. The results for the application of this platform to blood serum samples from stratified postliver transplant and nontransplant patients comparing both recurrent and persistent fibrosis progression illustrate that accurate detection and identification of larger panels of protein markers, rather than more limited individual biomarkers, is feasible with this platform and can potentially aid in the tracking and determination of disease progression.

The pursuit of future medical techniques such as personal profiling will likely require a broadening of potential diagnostic metrics, as partially demonstrated in the current study, where greater levels of detection for proteins and associated platforms will be key drivers. For example, early disease onset may be better detected by correlating an individual's protein abundances to a baseline panel established specifically for that person prior to disease onset instead of attempting to correlate a specific protein abundance value defined for an

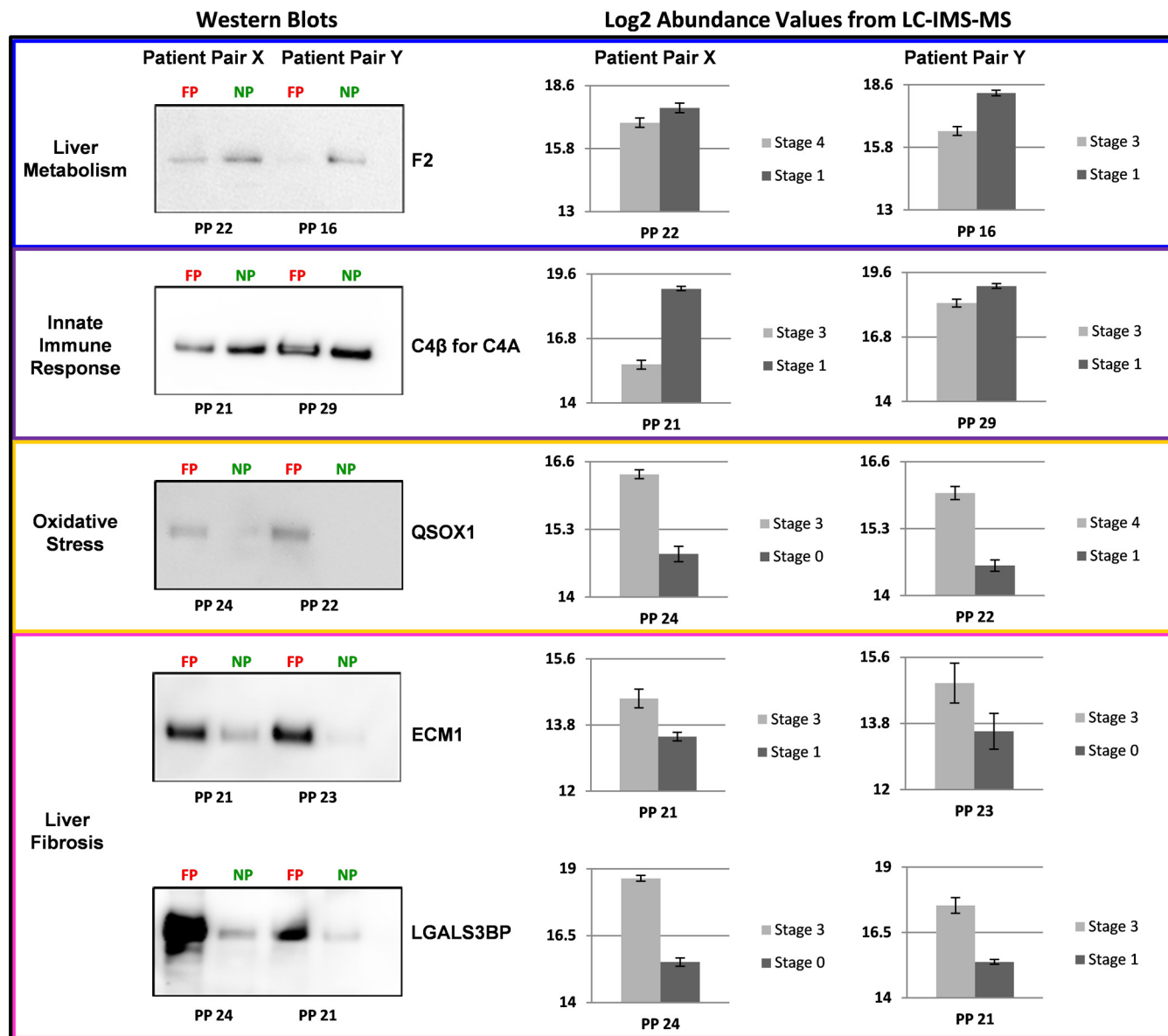


FIG. 5. Western blot (left) and LC-IMS-MS abundance (right) analyses of certain liver fibrosis patients where fast progressors (FP) were analyzed against their matched controls (NP) and patient fibrosis stage is noted on the bar graphs for the LC-IMS-MS abundance data. Patient pair is abbreviated as PP for clarity. For the Western blots an equal amount (5 μ g) of each serum protein sample was loaded. Targets were proteins involved in liver metabolism (F2: patient pairs 22 and 16), the innate immune system (C4A: patient pairs 21 and 29 (the Western targeted C4 β -chain, a cleavage product of C4A)), oxidative stress (QSOX1: patient pairs 24 and 22) and liver fibrosis (ECM1: patient pairs 21 and 23 and LGALS3BP: patient pairs 24 and 21).

entire population. This would of course require a broadly accepted protocol for routine serum collection and analysis of healthy people. Current MS approaches have technological advantages over immunoassays and/or similar technologies for analyzing multiple proteins simultaneously. Coupling the IMS separation to MS greatly increases measurement sensitivity while simultaneously reducing analysis time, leaving the IMS-MS platform as a key promoter of such an application in a clinical setting. However, we fully realize that this represents a paradigm shift in methodologies, and requires time and effort to develop the ancillary tools needed.

Acknowledgments—We thank Michael Perkins and Nathan Johnson for assistance in preparing the figures, Ryan Sontag for help with immunoblots, and Penny Colton for technical editing of the manuscript.

* A significant portion of this work was supported by the Washington State Life Sciences Discovery Fund. The development of the IMS-MS platform was provided through the National Institute of Health General Medical Sciences Proteomic Center at PNNL (2 P41 GM 103493-11) and other portions were supported by grants from the National Institute of General Medical Sciences (8 P41 GM103493-10), National Cancer Institute (R21-CA12619-01, U24-CA-160019-01, and Interagency Agreement Y01-CN-05013-29), National Institute of Environmental Health Sciences of the National Institutes of Health

(R01ES022190), the Entertainment Industry Foundation and its Women's Cancer Research Fund, the Laboratory Directed Research and Development Program at Pacific Northwest National Laboratory and by the Department of Energy Office of Biological and Environmental Research Genome Sciences Program under the Pan-omics project. The research was performed in the Environmental Molecular Science Laboratory, a U.S. Department of Energy (DOE) national scientific user facility at Pacific Northwest National Laboratory (PNNL) in Richland, WA. Battelle operates PNNL for the DOE under contract DE-AC05-76RLO01830.

☐ This article contains supplemental Tables S1 to S9.

||| These authors contributed equally.

✉ To whom correspondence should be addressed: Biological Sciences Division and Environmental Molecular Sciences Laboratory, 902 Battelle Blvd., P.O. Box 999, MSIN K8-98, Richland, WA 99352. Tel.: 509-371-6576; Fax: 509-371-6564; E-mail: rds@pnnl.gov.

REFERENCES

- Picotti, P., Rinner, O., Stallmach, R., Dautel, F., Farrah, T., Domon, B., Wenschuh, H., and Aebersold, R. (2010) High-throughput generation of selected reaction-monitoring assays for proteins and proteomes. *Nat. Methods* **7**, 43–46
- Addona, T. A., Abbatello, S. E., Schilling, B., Skates, S. J., Mani, D. R., Bunk, D. M., Spiegelman, C. H., Zimmerman, L. J., Ham, A. J., Keshishian, H., Hall, S. C., Allen, S., Blackman, R. K., Borchers, C. H., Buck, C., Cardasis, H. L., Cusack, M. P., Dodder, N. G., Gibson, B. W., Held, J. M., Hiltke, T., Jackson, A., Johansen, E. B., Kinsinger, C. R., Li, J., Mesri, M., Neubert, T. A., Niles, R. K., Pulsipher, T. C., Ransohoff, D., Rodriguez, H., Rudnick, P. A., Smith, D., Tabb, D. L., Tegeler, T. J., Variyath, A. M., Vega-Montoto, L. J., Wahlander, A., Waldemarson, S., Wang, M., Whiteaker, J. R., Zhao, L., Anderson, N. L., Fisher, S. J., Liebler, D. C., Paulovich, A. G., Regnier, F. E., Tempst, P., and Carr, S. A. (2009) Multi-site assessment of the precision and reproducibility of multiple reaction monitoring-based measurements of proteins in plasma. *Nat. Biotechnol.* **27**, 633–641
- Roschinger, W., Olgemoller, B., Fingerhut, R., Liebl, B., and Roscher, A. A. (2003) Advances in analytical mass spectrometry to improve screening for inherited metabolic diseases. *Eur. J. Pediatr.* **162**, S67–76
- Gallien, S., Duriez, E., and Domon, B. (2011) Selected reaction monitoring applied to proteomics. *J. Mass Spectrom.* **46**, 298–312
- Woodcock, J. (2007) The prospects for “personalized medicine” in drug development and drug therapy. *Clin. Pharmacol. Ther.* **81**, 164–169
- Chan, I. S., and Ginsburg, G. S. (2011) Personalized medicine: progress and promise. *Annu. Rev. Genomics Hum. Genet.* **12**, 217–244
- Hutchinson, L. (2011) Personalized cancer medicine: era of promise and progress. *Nat. Rev. Clin. Oncol.* **8**, 121
- Shen, Y. F., Zhao, R., Berger, S. J., Anderson, G. A., Rodriguez, N., and Smith, R. D. (2002) High-efficiency nanoscale liquid chromatography coupled on-line with mass spectrometry using nanoelectrospray ionization for proteomics. *Anal. Chem.* **74**, 4235–4249
- Mason, E., and McDaniel, E. (1988) *Transport Properties of Ions in Gases*, Wiley, New York
- Guevremont, R., Siu, K. W., Wang, J., and Ding, L. (1997) Combined ion mobility/time-of-flight mass spectrometry study of electrospray-generated ions. *Anal. Chem.* **69**, 3959–3965
- Sowell, R. A., Koeniger, S. L., Valentine, S. J., Moon, M. H., and Clemmer, D. E. (2004) Nanoflow LC/IMS-MS and LC/IMS-CID/MS of protein mixtures. *J. Am. Soc. Mass Spectrom.* **15**, 1341–1353
- Baker, E. S., Livesay, E. A., Orton, D. J., Moore, R. J., Danielson, W. F., 3rd, Prior, D. C., Ibrahim, Y. M., LaMarche, B. L., Mayampurath, A. M., Schepmoes, A. A., Hopkins, D. F., Tang, K., Smith, R. D., and Belov, M. E. (2010) An LC-IMS-MS platform providing increased dynamic range for high-throughput proteomic studies. *J. Proteome Res.* **9**, 997–1006
- Livesay, E. A., Tang, K., Taylor, B. K., Buschbach, M. A., Hopkins, D. F., LaMarche, B. L., Zhao, R., Shen, Y., Orton, D. J., Moore, R. J., Kelly, R. T., Udseth, H. R., and Smith, R. D. (2007) Fully automated four-column capillary LC–MS system for maximizing throughput in proteomic analyses. *Anal. Chem.* **80**, 294–302
- Tang, K., Shvartsburg, A. A., Lee, H. N., Prior, D. C., Buschbach, M. A., Li, F., Tolmachev, A. V., Anderson, G. A., and Smith, R. D. (2005) High-sensitivity ion mobility spectrometry/mass spectrometry using electrodynamic ion funnel interfaces. *Anal. Chem.* **77**, 3330–3339
- Belov, M. E., Buschbach, M. A., Prior, D. C., Tang, K., and Smith, R. D. (2007) Multiplexed ion mobility spectrometry-orthogonal time-of-flight mass spectrometry. *Anal. Chem.* **79**, 2451–2462
- Clowers, B. H., Belov, M. E., Prior, D. C., Danielson, W. F., 3rd, Ibrahim, Y., and Smith, R. D. (2008) Pseudorandom sequence modifications for ion mobility orthogonal time-of-flight mass spectrometry. *Anal. Chem.* **80**, 2464–2473
- Llovet, J. M., Burroughs, A., and Bruix, J. (2003) Hepatocellular carcinoma. *Lancet* **362**, 1907–1917
- Charlton, M., Ruppert, K., Belle, S. H., Bass, N., Schafer, D., Wiesner, R. H., Detre, K., Wei, Y., and Everhart, J. (2004) Long-term results and modeling to predict outcomes in recipients with HCV infection: results of the NIDDK liver transplantation database. *Liver Transpl.* **10**, 1120–1130
- Thomson, B. J., and Finch, R. G. (2005) Hepatitis C virus infection. *Clin. Microbiol. Infect.* **11**, 86–94
- Mukherjee, S., and Sorrell, M. F. (2006) Noninvasive tests for liver fibrosis. *Semin. Liver Dis.* **26**, 337–347
- Plebani, M., and Basso, D. (2007) Non-invasive assessment of chronic liver and gastric diseases. *Clin. Chim. Acta* **381**, 39–49
- Polpitiya, A. D., Qian, W. J., Jaitly, N., Petyuk, V. A., Adkins, J. N., Camp, D. G., 2nd, Anderson, G. A., and Smith, R. D. (2008) DANTE: a statistical tool for quantitative analysis of -omics data. *Bioinformatics* **24**, 1556–1558
- Diamond, D. L., Jacobs, J. M., Paepfer, B., Proll, S. C., Gritsenko, M. A., Carithers, R. L., Jr., Larson, A. M., Yeh, M. M., Camp, D. G., 2nd, Smith, R. D., and Katze, M. G. (2007) Proteomic profiling of human liver biopsies: hepatitis C virus-induced fibrosis and mitochondrial dysfunction. *Hepatology* **46**, 649–657
- Imakire, K., Uto, H., Sato, Y., Sasaki, F., Mawatari, S., Ido, A., Shimoda, K., Hayashi, K., Stuver, S. O., Ito, Y., Okanou, T., and Tsubouchi, H. (2012) Difference in serum complement component C4a levels between hepatitis C virus carriers with persistently normal alanine aminotransferase levels or chronic hepatitis C. *Mol. Med. Report* **6**, 259–264
- Banerjee, A., Mazumdar, B., Meyer, K., Di Bisceglie, A. M., Ray, R. B., and Ray, R. (2011) Transcriptional repression of C4 complement by hepatitis C virus proteins. *J. Virol.* **85**, 4157–4166
- Martin, M., Lefaix, J. L., Pinton, P., Crechet, F., and Daburon, F. (1993) Temporal modulation of TGF-beta 1 and beta-actin gene expression in pig skin and muscular fibrosis after ionizing radiation. *Radiat. Res.* **134**, 63–70
- Jablonska, E., Markart, P., Zakrzewicz, D., Preissner, K. T., and Wygrecka, M. (2010) Transforming growth factor-beta1 induces expression of human coagulation factor XII via Smad3 and JNK signaling pathways in human lung fibroblasts. *J. Biol. Chem.* **285**, 11638–11651
- Scotton, C. J., Krupiczkoj, M. A., Konigshoff, M., Mercer, P. F., Lee, Y. C., Kaminski, N., Morser, J., Post, J. M., Maher, T. M., Nicholson, A. G., Moffatt, J. D., Laurent, G. J., Derian, C. K., Eickelberg, O., and Chambers, R. C. (2009) Increased local expression of coagulation factor X contributes to the fibrotic response in human and murine lung injury. *J. Clin. Invest.* **119**, 2550–2563
- Hillebrandt, S., Wasmuth, H. E., Weiskirchen, R., Hellerbrand, C., Keppeler, H., Werth, A., Schirin-Sokhan, R., Wilkens, G., Geier, A., Lorenzen, J., Kohl, J., Gressner, A. M., Matern, S., and Lammert, F. (2005) Complement factor 5 is a quantitative trait gene that modifies liver fibrogenesis in mice and humans. *Nat. Genet.* **37**, 835–843
- Qin, S., Zhou, Y., Lok, A. S., Tsodikov, A., Yan, X., Gray, L., Yuan, M., Moritz, R. L., Galas, D., Omenn, G. S., and Hood, L. (2012) SRM targeted proteomics in search for biomarkers of HCV-induced progression of fibrosis to cirrhosis in HALT-C patients. *Proteomics* **12**, 1244–1252
- Cheung, K. J., Libbrecht, L., Tilleman, K., Deforce, D., Colle, I., and Van Vlierberghe, H. (2010) Galectin-3-binding protein: a serological and histological assessment in accordance with hepatitis C-related liver fibrosis. *Eur. J. Gastroenterol. Hepatol.* **22**, 1066–1073
- Cheung, K. J., Tilleman, K., Deforce, D., Colle, I., Moreno, C., Gustot, T., and Van Vlierberghe, H. (2011) Usefulness of a novel serum proteome-derived index FI-PRO (fibrosis-protein) in the prediction of fibrosis in chronic hepatitis C. *Eur. J. Gastroenterol. Hepatol.* **23**, 701–710
- Bell, L. N., Theodorakis, J. L., Vuppalanchi, R., Saxena, R., Bemis, K. G., Wang, M., and Chalasani, N. (2010) Serum proteomics and biomarker discovery across the spectrum of nonalcoholic fatty liver disease. *Hepatology* **51**, 111–120